Marine Mammal Science

MARINE MAMMAL SCIENCE, 00(00): 1–26 (2018)

DOI: 10.1111/mms.12544

Whales from space: Four mysticete species described using new VHR satellite imagery

Hannah C. Cubaynes,[1] British Antarctic Survey, Madingley Road, Cambridge CB3 0ET, United Kingdom and Scott Polar Research Institute, Department of Geography, University of Cambridge, Lensfield Road, Cambridge, CB2 1ER, United Kingdom; **Peter T. Fretwell,** British Antarctic Survey, Madingley Road, Cambridge, CB3 0ET, United Kingdom; **Connor Bamford,** British Antarctic Survey, Madingley Road, Cambridge, CB3 0ET, United Kingdom and University of Southampton, University Road, Southampton, SO17 1BJ, United Kingdom; **Laura Gerrish** and **Jennifer A. Jackson,** British Antarctic Survey, Madingley Road, Cambridge, CB3 0ET, United Kingdom.

Abstract

Large-bodied animals such as baleen whales can now be detected with very high resolution (VHR) satellite imagery, allowing for scientific studies of whales in remote and inaccessible areas where traditional survey methods are limited or impractical. Here we present the first study of baleen whales using the WorldView-3 satellite, which has a maximum spatial resolution of 31 cm in the panchromatic band, the highest currently available to nonmilitary professionals. We manually detected, described, and counted four different mysticete species: fin whales (*Balaenoptera physalus*) in the Ligurian Sea, humpback whales (*Megaptera novaeangliae*) off Hawaii, southern right whales (*Eubalaena australis*) off Península Valdés, and gray whales (*Eschrichtius robustus*) in Laguna San Ignacio. Visual and spectral analyses were conducted for each species, their surrounding waters, and nonwhale objects (*e.g.*, boats). We found that behavioral and morphological differences made some species more distinguishable than others. Fin and gray whales were the easiest to discern due to their contrasting body coloration with surrounding water, and their prone body position, which is proximal to the sea surface (*i.e.*, body parallel to the sea surface). These results demonstrate the feasibility of using VHR satellite technology for monitoring the great whales.

Key words: remote sensing, VHR satellite imagery, mysticete, baleen whale, *Balaenoptera physalus*, *Megaptera novaeangliae*, *Eubalaena australis*, *Eschrichtius robustus*.

Surveys that monitor whale populations are crucial for assessing abundance, density, distribution, and health status. These are particularly

[1]Corresponding author (e-mail: hcc57@cam.ac.uk).

important for whale populations recovering from historical harvests (Clapham and Baker 2002, Reeves and Smith 2003), and those influenced by anthropogenic impacts, including ship strikes (*e.g.*, fin whales, *Balaenoptera physalus*; Laist *et al.* 2001, IWC 2011, Vaes and Druon 2013) and fishing gear entanglement (*e.g.*, right whales, *Eubalaena*; Knowlton *et al.* 2012, IWC 2011). Currently, nine out of the 14 known baleen whale species (*e.g.*, fin whale) are recorded on the IUCN Red List either in one of the threatened categories (*i.e.*, critically endangered, endangered, and vulnerable) or as data deficient (IUCN 2017). Therefore, for the majority of baleen whale species, there is a strong conservation-based rationale for developing new technology to monitor abundance and distribution (Reilly *et al.* 2008, 2013).

Whale population sizes and distributions are traditionally assessed using boat, land, or aerial survey platforms (*e.g.*, Donovan and Gunnlaugsson 1989, Hiby and Hammond 1989, Buckland *et al.* 2001). Since most baleen whales are seasonally migratory (Rugh *et al.* 2001, Mate and Urbán-Ramirez 2003, Rasmussen *et al.* 2007, Jefferson *et al.* 2015), vast oceanic areas must often be surveyed to build a good understanding of migratory routes, distribution, abundance, and habitat use in different seasonal habitats. Some mysticete species inhabit remote areas not easily accessed by boat or plane (Nieukirk *et al.* 2004, Mellinger *et al.* 2007), such as Omura's whales (*B. omurai*) north of Madagascar (Cerchio *et al.* 2015) and sei whales (*B. borealis*) off the southern Chilean coast (Häussermann et al. 2017). The challenges of studying large and remote marine areas could potentially be assisted by utilizing the existing VHR satellites orbiting the Earth (Abileah 2002, Fretwell *et al.* 2014, McMahon *et al.* 2014, LaRue *et al.* 2017).

VHR satellites generate Earth surface images with submeter spatial resolution, meaning objects the size of great whales (*i.e.*, 10–33 m) can be observed on satellite images (Fretwell *et al.* 2014). Abileah (2002) tested this concept with the IKONOS 2 satellite to census marine mammals. The IKONOS 2 satellite provided images with a spatial resolution of 82 cm in the panchromatic band (*i.e.*, black and white image) and 3.2 m in the multispectral band (*i.e.*, color image; Abileah 2002). On one of the examined images, objects were identified as probable humpback whales (*Megaptera novaeangliae*) due to their size, and the location and time that the image was acquired. A decade later, the WorldView-2 was launched and offered higher spatial resolution (50 cm panchromatic and 1.84 m multispectral) than IKONOS 2. Fretwell *et al.* (2014) detected southern right whales (*E. australis*), both manually and automatically, with WorldView-2 satellite imagery, demonstrating the utility of satellite image technology for detecting great whales (*i.e.*, sperm whales, *Physeter microcephalus*, and baleen whales).

Since Fretwell *et al.* (2014), a new satellite now orbits the Earth, the WorldView-3, which provides the highest spatial resolution available to date (31 cm panchromatic and 1.24 m multispectral). In terms of pixels per surface area, the number has more than doubled, from 4.3 pixels filling 1 m^2 in a 46 cm resolution image (*e.g.*, WorldView-2, and GeoEye-1 satellites) to 9.4 pixels per m^2 for a 31 cm resolution image. For whales, it means that characteristic features such as flippers and flukes, not

easily detected on 46 cm resolution images, can be seen more clearly on 31 cm resolution images. Based on the morphometric measurements given by Woodward *et al.* (2006), the fluke surface area of an average sized gray whale takes up about six pixels on a 46 cm resolution image, whereas on a 31 cm resolution image it is comprised of approximately 10 pixels. The ability to differentiate the body outline and features (*e.g.*, fluke) is approximately 1.6 times better with WorldView-3 imagery. The capability of reliably distinguishing characteristic features of whales is essential for identifying an object as a whale, and for differentiating species.

Development of a satellite-based, automated whale detection system requires capturing images that clearly allow identification of different whale species, before questions involving aspects of population biology can be addressed. Comparative species identification remains untested for satellite images, thus, we make the first attempt to characterize the unique spectral signature (*i.e.*, the shape of the spectral reflectance curve), and characteristic features of four whale species found in different marine habitats. With the support of WorldView-3 images, our study focuses on (1) identifying the unique visual characteristics and spectral signature of the focal whale species and (2) developing a method to count whales manually and to categorize counts by level of confidence.

Four highly distinguishable species were targeted for this study (Perrin *et al.* 2009, Jefferson *et al.* 2015), including the fin whale in the Pelagos Sanctuary (France, Monaco, and Italy), the humpback whale off Maui Nui (Hawaii), the southern right whale off Península Valdés (Argentina), and the gray whale (*Eschrichtius robustus*) in Laguna San Ignacio (Mexico). Each species has been well studied on either their feeding or breeding grounds (Rowntree *et al.* 2001, Urbán *et al.* 2003, Herman *et al.* 2011, Panigada *et al.* 2011, Ponce *et al.* 2012) where they occur in relatively high abundance, making the study of each species using VHR satellite technology feasible. Spectral analyses of each species, their surrounding waters, and other nonwhale objects were subsequently conducted to ascertain the signatures are unique to each species in WorldView-3 images. Results of this survey contribute towards the development of an automated detection system that may be able to distinguish whale species and count them from space.

Methods

Image Selection

WorldView-3 satellite images were collected from four known baleen whale habitats (Fig. 1). Images were acquired from DigitalGlobe, WorldView-3 imagery provider. All images had a spatial resolution of 31 cm for the panchromatic band (*i.e.*, black and white image) and 1.24 m for the multispectral bands (*i.e.*, color image). Four multispectral bands were acquired for all locations (*i.e.*, blue, green, red, and near infrared 1 (NIR1); DigitalGlobe 2017). The choice of species, and location and time of acquisition of the satellite images was based on the following four prime criteria: (1) morphological differences: the candidate

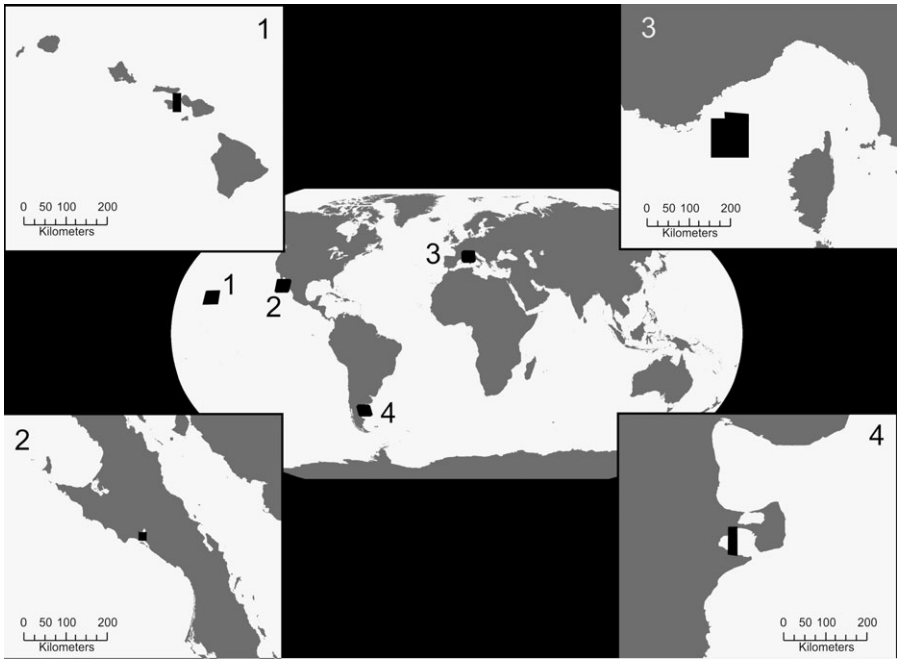

Figure 1. Locations of study areas: (1) Maui Nui in the United States of America, (2) Laguna San Ignacio in Mexico, (3) Pelagos Sanctuary in the Ligurian Sea, and (4) Península Valdés in Argentina. Black shapes in the four subareas represent the extent of the satellite imagery acquired and used in this study.

species are morphologically distinct from each other and from other great whale species; (2) whale abundance: to optimize the likelihood of whales being present at the sea surface in the images, images were collected near the known peak in seasonal abundance for each species; (3) sea surface conditions: ideal conditions to observe whales on satellite imagery are few or no white caps, low glare, and low swell (see Fretwell *et al.* (2014) and Abileah (2002) for details about limitations in manual detection of whales in rough sea state on satellite imagery); and (4) other megafauna: the image locations and times were chosen so that no other large marine animals (*e.g.*, Bryde's whales, *B. edeni*) of similar size to the studied whales (*e.g.*, fin whales) were likely to be present at the time the images were taken. Although changes in whale distribution are predicted (Learmonth *et al.* 2006, Schumann *et al.* 2013, Silber *et al.* 2017), or have already happened for some species (Ramp *et al.* 2015), no other marine mammals similar in size to the target species have yet been reported to regularly occur during the periods that satellite images were collected for this study.

At location 1 (Fig. 1), one satellite image (570 km^2) of the Au'au Channel in Maui Nui, Hawaii, taken on 9 January 2015 was acquired from DigitalGlobe archives. This region is a well known humpback whale

breeding ground from December to April with peak abundance between February and March (Mobley *et al.* 2001, Herman *et al.* 2011, Baird *et al.* 2015). No other marine mammals similar in size to humpback whales are regularly reported in Maui Nui during this season. Rarely, blue whales (*B. musculus*), fin whales, minke whales (*B. acutorostrata*), sei whales, and Bryde's whales have been sighted offshore, north of the main Hawaiian Islands (*i.e.*, outside and north of the Au'au Channel; Mobley *et al.* 2000, Barlow 2006, Smultea *et al.* 2010). Although sperm whales have been recorded in the region, they tend to stay in deep water away from the main Hawaiian Islands (Mobley *et al.* 2000, Barlow 2006). Based on OBIS-SEAMAP data (Halpin *et al.* 2009). The probability of observing one of these species within the acquired satellite image was negligible. Therefore, we assumed that only humpback whales were present in the analyzed satellite image. The Au'au Channel is partly enclosed by four islands, and therefore has low swell and provides ideal sea surface conditions for satellite imagery analysis.

At location 2 (Fig. 1), one satellite image (80 km^2) of Laguna San Ignacio, Mexico, was actively collected on 20 February 2017, which coincides with the calving season for gray whales (Jones and Swartz 1984, Urbán *et al.* 2003). Although humpback whales and blue whales (*B. musculus*) are encountered off the coast of Baja California during winter, no sightings have been reported within Laguna San Ignacio (Urbán and Aguayo 1987, Steiger *et al.* 1991, Mate *et al.* 1999, Calambokidis and Barlow 2004, Bailey *et al.* 2009). Based on OBIS-SEAMAP data (Halpin *et al.* 2009), the probability of encountering whale species other than gray whales was negligible. Therefore, we assumed that only gray whales were present in the analyzed satellite image. Laguna San Ignacio is a small, enclosed area, where the swell was expected to be low.

At location 3 (Fig. 1), four satellite images (4,230 km^2) were actively collected for a region of the Pelagos Sanctuary in the Mediterranean Sea, spanning French, Monégasque, and Italian waters. Three were taken on 19 June 2016 and one was acquired on 26 June 2016. In the summer, fin whales are known to be present in the deep western offshore water of this sanctuary (Forcada *et al.* 1995, Notarbartolo di Sciara *et al.* 2003, Panigada *et al.* 2011). The choice of location for the images was based on the findings of Panigada *et al.* (2008) who used habitat models to identify an area where fin whale abundance was likely to be the highest. In the Pelagos Sanctuary no other large marine animals similar in size to the Mediterranean fin whale (*i.e.*, maximum body length of 24 m) have been observed with any regularity or in high abundance. Sperm whales (*i.e.*, maximum body length of 18 m) are usually found next to steep topographic features such as canyons, some of which are located near the northern edge of the studied images (Moulins *et al.* 2008, Jefferson *et al.* 2015). Based on OBIS-SEAMAP data (Halpin *et al.* 2009, Lanfredi and Notarbartolo di Sciara 2011, Boisseau 2014, Lanfredi and Notarbartolo di Sciara 2014, Frey 2015, Van Canneyt 2016), there was a probability of 87% that a large whale species encountered in the acquired satellite image was a fin whale, and a probability of 13.04% that it was a sperm whale. The different body shape should limit misidentification between a fin whale (*i.e.*, sleek, streamlined) and a sperm whale (*i.e.*,

log-like; Jefferson *et al.* 2015). Whale-like objects observed on the images of the Pelagos were included in the visual and spectral analysis only if they had a streamlined body shape. In the northwestern Mediterranean Sea there have been rare observations of humpback whales (Frantzis *et al.* 2004, Dhermain *et al.* 2015) measuring a maximum of 18 m (Jefferson *et al.* 2015). Based on OBIS-SEAMAP data, the probability of observing a humpback whale within the boundaries on the acquired satellite images was negligible. Therefore, we assumed only fin whales were present in the analyzed satellite image. Summer sea conditions in the northern Mediterranean are characterized by calm sea conditions (Panigada *et al.* 2008). Due to the size and enclosed nature of the Mediterranean basin, the swell was expected to be lower than that in the open ocean.

At location 4 (Fig. 1), one satellite image (560 km^2) taken on 16 October 2014 of Golfo Nuevo in Península Valdés, Argentina, was acquired from DigitalGlobe archives. It coincides with the calving season for the southern right whales. During the past four decades that their population has been monitored, southern right whales inhabit Península Valdés between May and December, with peak abundance from mid-August until early October (Payne 1986, Cooke *et al.* 2015, IWC 2013, Crespo *et al.* 2014). Based on OBIS-SEAMAP data (Halpin *et al.* 2009), the probability of encountering any other large whale species was null. Although killer whales (*Orcinus orca*) are the only other large marine mammal known to enter this bay, they are much smaller than southern right whales and arrive later, around December (Iñiguez 2001). Consequently, we assumed only southern right whales could be observed on the analyzed satellite image. Regarding the sea surface conditions required for satellite imagery analysis, Golfo Nuevo is sheltered and relatively calm sea conditions were expected compared to the open ocean.

Visual Image Analysis

One observer, experienced in whale identification at sea, visually identified and manually counted all large whale species on each satellite image. Throughout this manuscript, whale identification on satellite imagery refers to the classification of an object as a whale. The manual counting method involved loading all acquired satellite images into ArcGIS 10.4 ESRI 2017. To improve whale detectability, pan-sharpened images (*i.e.*, high resolution color images) were created using the ESRI algorithm in ArcGIS 10.4 ESRI 2017. This algorithm combined the low resolution multispectral images (*i.e.*, 1.24 m) with the high resolution panchromatic images (*i.e.*, 31 cm) to generate high resolution multispectral images (*i.e.*, 31 cm). Each pan-sharpened image was manually and systematically scanned using a grid system at a scale of 1:1,500 m. Detected objects needing more scrutiny were looked at a higher scale (*e.g.*, 1:500). To scan an area of 100 km^2 took approximately 3 h and 20 min.

Determining if an object was a whale, and accounting for the confidence of the observer in the identification of whale-like objects, involved the use of a classification method (see Appendix S1). The classification

was trialed using two additional observers in order to check for consistency and identify any classification parameters that vary between observers. A random subset of 10 whale-like objects per species was provided to both observers (see Appendix S1). The classification allowed categorizing each whale-like object as "definite," "probable," "possible." The proportion of "definite" whales among all counted whales (*i.e.*, including "probable" and "possible" individuals) was calculated for each candidate species.

A selection of whale-like objects classified as "definite" were used to describe obvious morphological differences among species when viewed from space. The following anatomy, if visible, was measured in ArcGIS 10.4 ESRI 2017: (1) body length (A in Table 1), (2) body width (B in Table 1), (3) flipper length (C in Table 1), (4) fluke width (D in Table 1). Mean and standard deviation were calculated for all measured anatomy, then compared to known measurements of large whale species (Jefferson *et al.* 2015). Characterization of surface and near surface water disturbances associated with each species was also recorded (Table 2). Boats and planes were also recorded as nonwhale objects.

Spectral Image Analysis

One of the motives of this research was also to assess what parameters can be helpful when attempting to automate the detection of whales on satellite images. Each pixel of a satellite image contains quantifiable information (Rees 2013), not visible to the human eye. A human eye can only see the red, blue, and green wavelengths of the electromagnetic spectrum (Nathans *et al.* 1986), whereas sensors on the WorldView-3 satellite can detect additional wavelengths of the electromagnetic spectrum (DigitalGlobe 2017). The sensors of the WorldView-3 also assign a value to each of the wavelength ranges it can detect (*i.e.*, each multispectral band), which the human eye cannot see. The assigned value is called the spectral radiance ($W \cdot m^{-2} \cdot sr^{-1} \cdot \mu m^{-1}$). It is the amount of light reflected by the target for a specific wavelength (Rees 2013). Each pixel from the WorldView-3 satellite images acquired for this study held four radiances, one for each of the multispectral bands, or wavelength ranges: blue (450–510 nm), green (510–580 nm), red (630–690 nm) and NIR1 (770–895 nm; DigitalGlobe 2017).

Spectral analysis was performed on each image to characterize each whale species, and to investigate if and how they differ from each other, their surrounding environments, and nonwhale objects (*e.g.*, boats and planes). First, we corrected the multispectral image of each location for the top of atmosphere using ENVI software (Harris Geospatial). The top of atmosphere correction is a necessary step before analyzing the radiances of surfaces and objects on the Earth. Without this correction, a satellite image will show the overall radiance value of the surfaces and the particles contained in the atmosphere (Rees 2013). Then, we extracted the four radiances for each pixel of whale-like objects, water and nonwhale objects from the satellite image.

Table 1. Summary of morphological characteristics per surveyed species.

Species	Number of "definite" whales	Number of "probable" whales	Number of "possible" whales	Total number of whales	Proportion of definite whale (%)	Average body measurements (m)[b]	Distinctive characteristics
Fin whale	26	3	5	34	76.47	A: 13.49 (n = 9, SD = 2.92) B: 2.56 (n = 9, SD = 0.47) C: 1.94 (n = 6, SD = 0.23) D: 3.68 (n = 1, SD = NA)	Streamlined body
Southern right whale	23	12	23 (1)[a]	59	38.98	A: 10.47 (n = 6, SD = 2.69) B: 3.08 (n = 6, SD = 0.39) C: NA (n = 0, SD = NA) D: 4.45 (n = 1, SD = NA)	White callosities on the head
Humpback whale	20	11	25	56	35.71	A: 10.62 (n = 5, SD = 1.36) B: 2.94 (n = 4, SD = 0.43) C: 2.39 (n = 4, SD = 0.53) D: NA (n = 0, SD = NA)	Long flippers
Gray whale	27 (2)[a]	18 (4)[a]	17 (2)[a]	62	43.55	A: 12.58 (n = 10, SD = 0.95) B: 2.90 (n = 9, SD = 0.44) C: 1.90 (n = 3, SD = 0.27) D: 3.06 (n = 8, SD = 0.26)	Pale, whitish body

[a]Number of calves.
[b]A: body length, B: body width, C: flipper length, D: fluke width.

Table 2. Catalog of the different surface water disturbances and near surface disturbances associated with the four candidate whale species. All images are pan-sharpened. In the images where more than one sign are present, a red circle highlight the sign being referred to.

Sign	Description	Fin whale	Southern right whale	Humpback whale	Gray whale
After-breach	Large white area left after a whale breached, or lobtailed, flipper-slapped	Not observed on the studied satellite images	Not observed on the studied satellite images	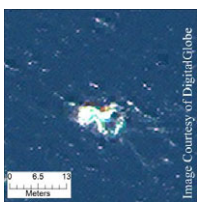	Not observed on the studied satellite images
Blow	Vaporous whitish patch next to a whale, similar looking to fog	Not observed on the studied satellite images	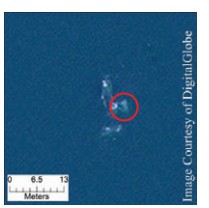	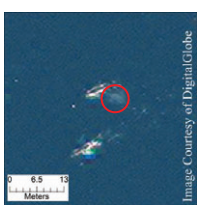	
Contour	White line separating the part of the whale body that is above and below the sea surface (*e.g.*, when a whale is rolling its back or surfacing to breathe)		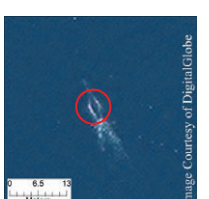	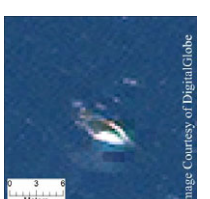	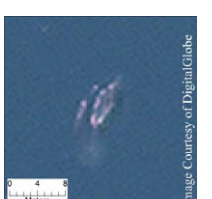

(Continues)

Table 2. Continued

Sign	Description	Fin whale	Southern right whale	Humpback whale	Gray whale
Flukeprint	White circle left after whale dove or while swimming (Levy *et al.* 2011)	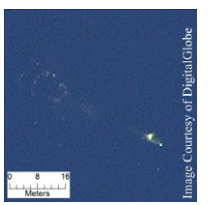	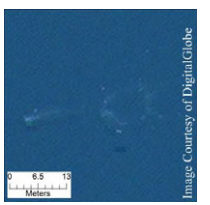	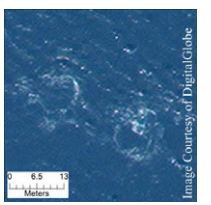	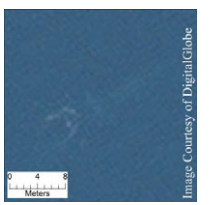
Wake	V-shaped white trail behind the animal	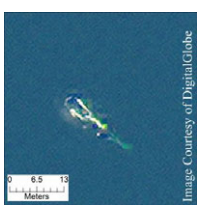	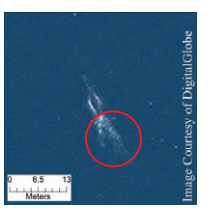	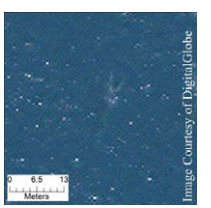	Not observed on the studied satellite images
Defecation	Trail of colored clouds behind animal	Not observed on the studied satellite images	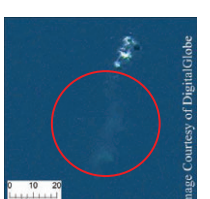	Not observed on the studied satellite images	Not observed on the studied satellite images

The radiance of whale-like objects was collected only for "end members." In remote sensing "end members" refers to a group of pure pixels (*e.g.*, pixels filled with whale only) as opposed to mixed pixels (*e.g.*, pixels filled with water and whale; Rees 2013). In this study, the "end members" were chosen among the "definite" individuals. The whales showing most of their body length were selected. Following this, we identified the pure pixels of every selected "definite" whales by describing every pixel of the selected "definite" whales with one, or a combination of the characteristics listed in Appendix S2. Some pixels were made of both water and submerged whale, or submerged whale and nonsubmerged whale (*i.e.*, mixed pixels). We removed these mixed pixels from the analysis, as they could bias the spectral analysis, and only retained the purest "whale pixels" (*i.e.*, only submerged whale, or only nonsubmerged whale).

The radiance of the surrounding environment of whales (*i.e.*, water) was assessed by manually selecting 100 pure pixels of water for each location, in clusters of five pixels. None of these pixels contained either white caps, or shallow water (*i.e.*, where the seabed was visible and the sea was lighter in color than the surrounding waters).

For nonwhale objects, we separately measured the radiance of boats and planes. For each type of nonwhale object (*i.e.*, boats or planes), 100 pure pixels were selected manually in clusters of five among all the counted objects.

For the acquisition of the radiance of whale-like objects, surrounding environments, and nonwhale objects, we used ArcGIS 10.4 ESRI 2017. The radiance was averaged for each whale species, and per location, for each type of nonwhale object and the surrounding waters. To allow for quantitative comparisons to be made between species, between whale-like and nonwhale objects, and between whale-like objects and their surrounding waters, the standard error of the mean was also calculated for each pixel set.

Results

Whale Morphology and Behavior

A total of 211 whale-like objects were observed across the four studied areas, covering approximately 5,440 km^2 (Table 1). Individuals of each of the four species were detected within their respective satellite images by manual scanning (Fig. 2). Most of the individuals identified were adults with the exception of gray whale calves (two "definite," four "probable," and two "possible") and one "possible" southern right whale calf. In terms of confidence in identification of an object as a whale, fin whales had the highest proportion of "definite" individuals, followed by gray whales, with humpback and southern right whales having the lowest proportion (Table 1). Comparison of the classification system between observers showed consensus in terms of whale identification when more subjective parameters (*e.g.*, body color) were down weighted (Appendix S1). There was no change in definite identifications for humpback whales and fin whales between the consensus

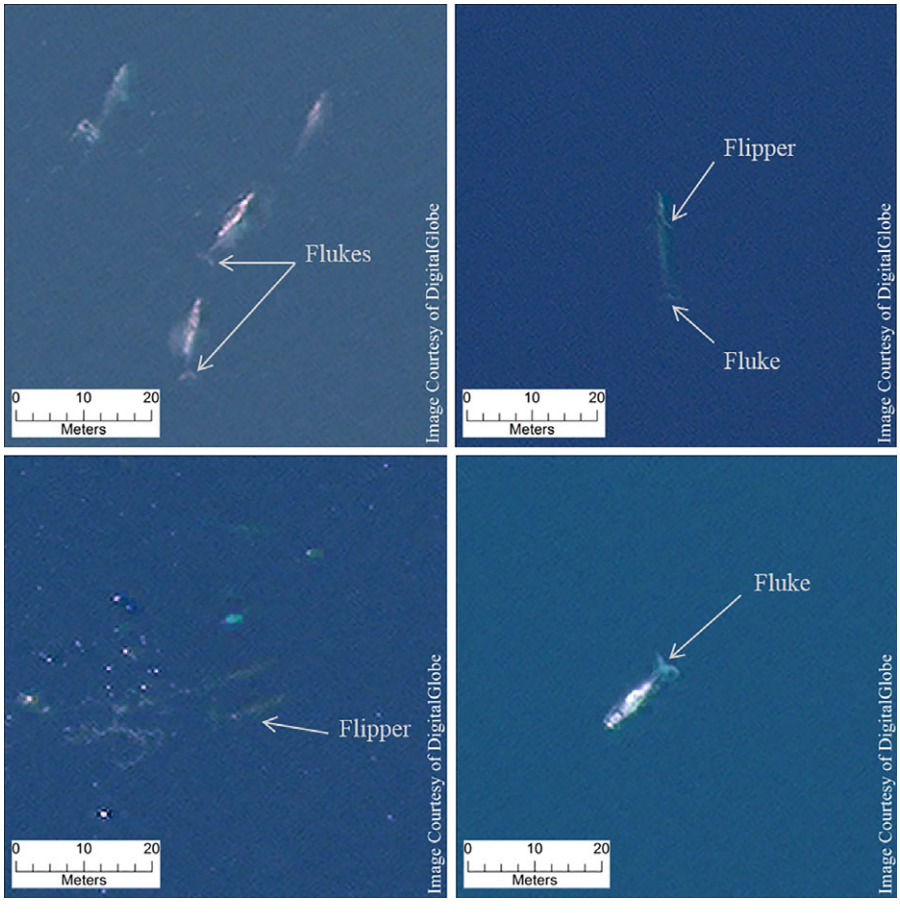

Figure 2. Pan-sharpened WorldView-3 satellite images of four "definite" gray whales in Laguna San Ignacio (top left), a "definite" fin whale in the Pelagos Sanctuary (top right), two "definite" humpback whales in Maui Nui (bottom left), and a "definite" southern right whale in Península Valdés (bottom right).

identification (*i.e.*, three observers) and the single observer identification. For gray whales and southern right whales, there were 10% less definite identifications when the consensus identification was used, than when a single observer was used (Appendix S1).

The total number of whale-like objects (categorized as "definite,", "probable," and "possible" whales) for fin whales included three individuals that were likely observed twice, as three of the four satellite images acquired for the Pelagos Sanctuary were taken on the same day with intervals of <30 s. These three whales were observed in the overlap region of these images in slightly different locations, suggesting movement. Among the 25 "possible" humpback whales, seven were included in this category based solely on the presence of whale signs, including flukeprints (Levy *et al.* 2011), that were not associated with any other

whales recorded in the image. These seven whale signs were estimated to be too far apart from any detected whales to be associated with them, and it is possible that they were associated with whales that dived too far below the surface to be visible on the satellite images.

The length and width measurements of the body were acquired for all the surveyed species. However, other body measurements such as flipper length or fluke width could not be measured for all individuals. No flukes were observed on any of the humpback whales, nor flippers for southern right whales (Table 1).

Some distinct body characteristics known to be unique features for each species were observed on some individuals, such as long flippers for the humpback whales; these were observed on five of the counted individuals. White head callosities, a characteristic specific to right whales, were positively identified on four of the recorded "definite" southern right whales (Table 1).

Along with body features, other evidence of whale presence was observed (Table 2). Some are related to surface water disturbance: after-breach, flukeprint, wake, and contour (see Table 2 for a description). There were also other signs associated with near surface disturbances: blow and defecation. Fluke prints and contours were observed for each surveyed species. Wake and blow were seen for three out of the four species. After-breach splashing was only detected for the humpback whale, likewise with defecation for the southern right whale.

Spectral Characteristics of Whales

The purest "whale pixels" that were retained for the spectral analyses were of submerged whales, as there were no pure pixels of whales above the sea surface for fin whales, gray whales, and humpback whales. There were six pure "whale pixels" of southern right whales below the sea surface, seven of humpback whales, 26 of gray whales, and 34 of fin whales. The spectral signatures of the four candidate species were overall similar in shape (Fig. 3). Comparatively, gray whales had the highest radiance values (*i.e.*, they were the lightest), followed closely by fin whales, then southern right whales and humpback whales, which are much darker (Fig. 3).

Comparisons of whale with their environment showed two main results: (1) the radiance values for gray whales and fin whales distinguished them from the surrounding waters of the location where they were studied, as well as the waters of the other study locations (Fig. 4); and (2) southern right whales and humpback whales had very similar radiance values relative to the surrounding waters of the location where they were studied, but were distinct relative to waters from other locations (Pelagos and San Ignacio; Fig. 4). Overall none of the spectral signatures of the four candidate species differed greatly from the spectral signatures of their environment (Fig. 4).

Nonwhale Objects

In all the analyzed satellite images, except the one from Península Valdés, nonwhale objects were observed and clearly discernible from

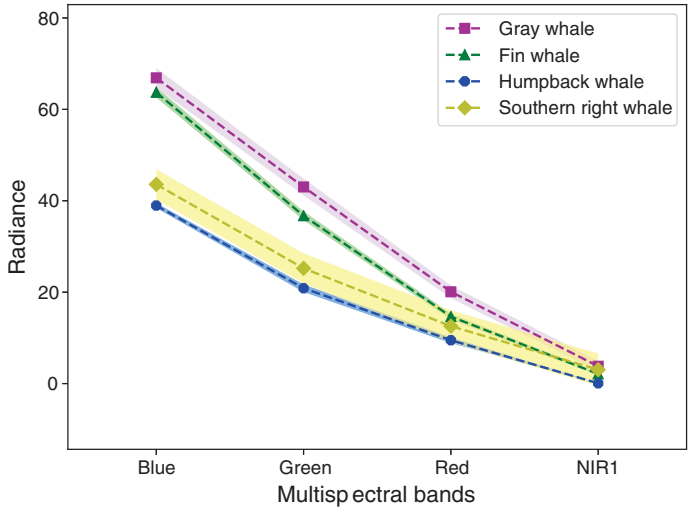

Figure 3. Radiance values of the four studied species for four multispectral bands. The shaded areas around the dotted lines correspond to the standard error of the mean.

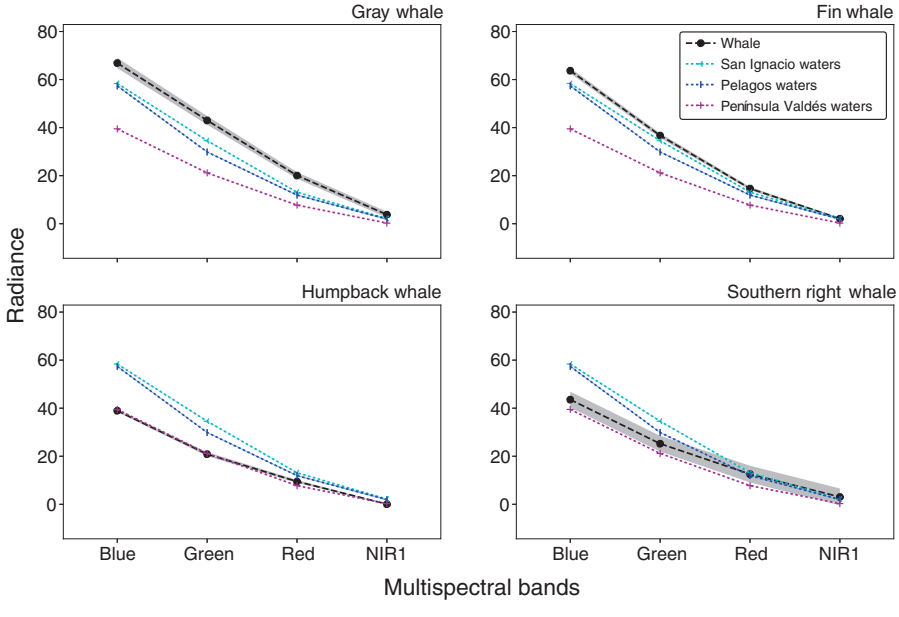

Figure 4. Radiance values of each candidate species compared to the radiance values of sea water of three of the four study locations. For clarity reasons, the waters off Maui Nui are not represented in this figure as their radiance values are fully overlapping with Península Valdés. The shaded areas around the dotted lines correspond to the standard error of the mean.

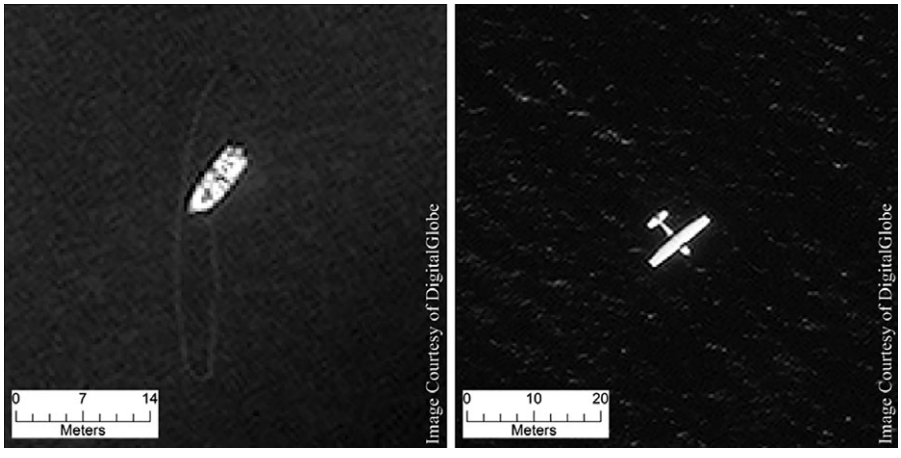

Figure 5. Panchromatic WorldView-3 satellite images of nonwhale objects: a fishing boat with visible net in Laguna San Ignacio (left) and a small aircraft in Maui Nui (right).

whale-like objects. Boats and planes were the only types of nonwhale objects that were detected (Fig. 5). Various types and sizes of boats were observed across the three locations (*i.e.*, the Pelagos Sanctuary, Laguna San Ignacio, and Maui Nui) such as ferries, fishing boats, cargo and sail boats. Planes, (*i.e.*, passenger and smaller aircraft) were detected in the Pelagos Sanctuary and Maui Nui. Among all the nonwhale objects that were observed, the ones of smaller or similar size to whales were confidently identified (and discriminated from whales) due to their recognizable shape and, sometimes, due to the presence of other features such as fishing gear (Fig. 5).

The spectral analysis of nonwhale objects demonstrated differences from whales in radiance values that could be used in an automated whale detection system. Boats and planes displayed higher radiance values than the gray, fin, and humpback whales (Fig. 6). The spectral signatures of the planes detected in the Pelagos Sanctuary showed a concave-down negative slope, compared to the fin whale spectral signature, which was comparatively straight (Fig. 6b). On the satellite image of Maui Nui, the planes exhibited a spectral signature similar to the humpback whales except for a slight plateau between the green and red bands (Fig. 6c). In comparison, boats were the only nonwhale object detected on the satellite image of Laguna San Ignacio (Fig. 6a). They showed a similar spectral signature to the gray whales, but could again be confidently discriminated due to their features.

Discussion

The four study species were detected on WorldView-3 satellite images, which are the first whale observations for this satellite system, and the first satellite-based detections of fin and gray whales. While earlier work

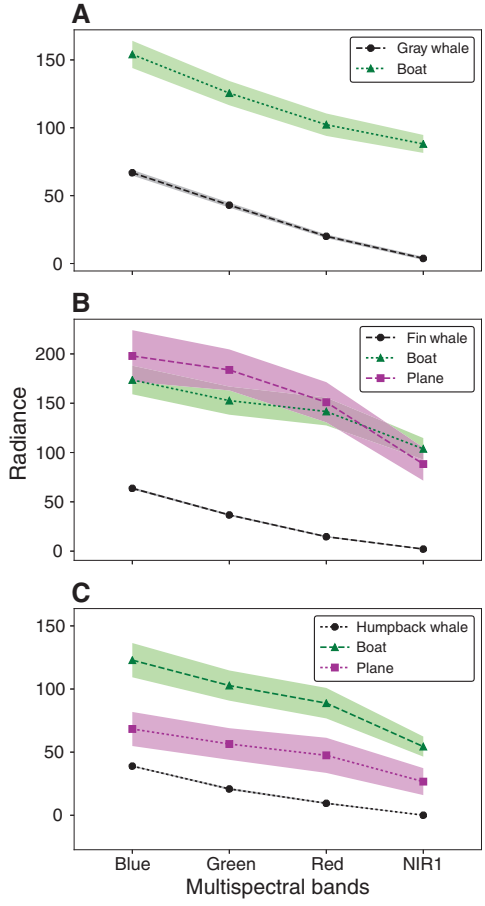

Figure 6. Radiance values of gray, fin, and humpback whales compared to the radiance values of nonwhale objects. (A) In the image of Laguna San Ignacio, boats were the only observed, nonwhale object. Graph (B) are the results for the Pelagos Sanctuary image and (C) for the image of Maui Nui. The shaded areas around the dotted lines correspond to the standard error of the mean.

detected right whales and probable humpback whales using Worldview-2 and IKONOS 2 satellite imagery, respectively (Abileah 2002, Fretwell *et al.* 2014), the higher spatial resolution of WorldView-3 made it possible to characterize each of the four surveyed species, and generate more confident observations. Characterizing each of these species was also possible due to the careful selection of time and location of acquisition of the imagery. Each image was taken when and where only one whale species was present, and near their respective peak abundance period.

Several characteristics helped identify objects as whales, including size, coloration, and specific features (*e.g.*, white head callosities, fluke). The size of the observed objects (*i.e.*, length and width) was the first

indication that an object could be a whale when compared to the known body size range (Shirihai and Jarrett 2006, Jefferson *et al.* 2015). In this study, gray whales were the only species found within their size range; all other species appeared smaller than expected. Adult southern right whales and humpback whales were close to the lower limit of their documented size range. The average body length of fin whales was below its known size range (Shirihai and Jarrett 2006, Jefferson *et al.* 2015). This discrepancy in body length compared to known size range is likely due to ascending or descending whales positioned diagonally to the sea surface. Additionally, flukes were rarely detected in the images of fin whales, southern right whales and humpback whales, which would lead to underestimates of body length. If there were doubts about the size of a whale-like object, other characteristics could be used to help identify whether it was a whale (*e.g.*, white head callosities). For instance, sea surface water disturbance such as flukeprints (Levy *et al.* 2011) were observed for all the studied species. Smaller details (*i.e.*, body features) also helped identify the observed objects as whales. Fluke and flippers were some of the main body features that could be observed among the four candidate species. Species-specific features were also observed and helped identify objects as whales, such as white head callosities which are distinctive of right whales for example. These smaller features, as well as body length and shape were, however, not equally seen for each species.

Identifying an object as a whale was more challenging for some species due to specific behaviors, which affect their detectability in the water. The "definite" observations were made when a whale was positioned parallel to the sea surface, which whales tend to do when traveling. In this position, body features such as fluke, flippers, as well as the general shape of the animal were visible. For example, the streamlined body shape could clearly be noticed for some fin whales and for gray whales with their more robust body. In contrast, the humpback whales were not as confidently identified. Their well-documented acrobatic nature on the breeding grounds (Helweg and Herman 1994, Frankel *et al.* 1995, Clapham and Mead 1999) hindered identification on the satellite image, as whale-specific characteristics such as body shape, flippers, or fluke were indistinct.

A strong contrast between a whale and its surrounding environments is required to detect whales on satellite imagery (LaRue *et al.* 2017). In comparison to humpback and southern right whales, fin and gray whales contrasted more strongly with their surrounding waters, with their light body coloration appearing a useful feature assisting identification. While Maui humpback whales and Península Valdés right whales did not show strong contrast in this study, more confident identifications may be made where they occur in lighter toned habitats, areas where the surrounding water is lighter in color. All species were clearly spectrally and visually distinct from nonwhale objects (*e.g.*, boats and planes), even though sizes were sometimes similar. Boats and planes, the only types of nonwhale objects observed on the satellite images, had clear specific outlines, different from whales. This dissimilarity was also seen in the spectral analysis with the different radiance values.

Although our study demonstrates that different species of large whales can be detected and counted using satellite images, manual scanning is time demanding. To reduce the time spent manually scanning satellite images, an automated system should be developed. The visual and spectral characterizations of the four study species could be used to inform and develop automated systems to detect them. Various methods currently exist to automatically identify specific objects (*e.g.*, Rees 2013, Fretwell *et al.* 2014, Maire *et al.* 2015). A common method used to analyze satellite images is based on a purely pixel analysis (*i.e.*, only the spectral characteristics) of a given object. Our results from the spectral analysis show that such a method is not likely to prove useful, as the four candidate species had similar spectral signatures with their habitat. However, other methods, such as an object-based image analysis (*e.g.*, Groom *et al.* 2011, Yang *et al.* 2014) or a deep learning approach (*e.g.*, Maire *et al.* 2015), may be more useful because these research techniques include the shape and texture of the object in addition to the spectral characteristics. The whale characteristics used to identify whale-like objects could be useful, particularly body shape and surface or near surface disturbances associated with a whale.

While a reliable automated detection method is under development, another way to reduce the time required to manually scan satellite images is to implement crowdsourcing projects (Supriadi and Prihatmanto 2016, Rey *et al.* 2017), requiring citizen scientists to scan the images and manually count the whales. One example of this approach is being taken for Weddell seals (*Leptonychotes weddellii*) on the Tomnod.com platform. However, for identification of whale signs, experienced marine mammal observers may be required, necessitating the careful set up of such a project. To maximize the utility of this approach, we recommend the following parameters to be considered when developing a satellite imagery based whale study (see Appendix S3 for more details): (1) behavior: *e.g.*, traveling or resting, which means the animal full body length will likely be parallel to the surface; (2) coloration relative to surrounding waters: *e.g.*, if observing a whale in deep water, lighter colors should be more easily discernible; (3) size: animal above 10 m in total length; (4) sea surface: *e.g.*, species found in calm coastal water compared to open ocean might be easier to detect due to a potentially lower swell; and (5) cooccurrence of similar species, *e.g.*, potential challenge for misidentification of species and potential for a positive bias in species-specific counts.

The constraint of animal size when using VHR satellite images to detect whales must be improved for broader applications. Spatial resolution of satellite images has improved since Abileah (2002), yet it does not appear to be high enough to detect smaller cetacean species or whale calves. In our study, two of the images were acquired during calving season, one for gray whales in Laguna San Ignacio (Jones and Swartz 1984, Urbán *et al.* 2003) and one for southern right whales in Península Valdés (Crespo *et al.* 2014, Cooke *et al.* 2015). Therefore, the presence of calves, which have an approximate length of 5 m for both species, was expected. However, few calves were observed on the satellite images and fewer with high confidence. This is likely explained by their

bodies being too small to clearly identify major anatomical features. Some of their behaviors, such as riding on the back of their mother, would also make it difficult to discern calves on VHR satellite images (Smultea *et al.* 2017).

As with the traditional survey methods, surface presence is an issue when surveying whale populations (Marsh and Sinclair 1989, Buckland and Turnock 1992, Buckland *et al.* 2001). Deep-diving species provide future challenges (to growth and density estimates) due to relatively lower sightings. Comparative studies between aerial and satellite-based methods are needed to assess the utility of satellite imagery for estimating density relative to aerial surveys. A better understanding of how deep below the sea surface a whale is likely to be visible on satellite images is also required. As suggested by Fretwell *et al.* (2014), large reflectance panels could be installed underwater in key habitats, to assist with calibrating the depth at which whales are visible. Another idea would be to install artificial whale models at various depths, similar to what Pollock *et al.* (2006) and Robbins *et al.* (2014) did with artificial dugong (*Dugong dugon*) and shark models to estimate the detectability of these animals from aircraft.

Per unit area, VHR satellite imagery has the potential to provide a cheaper and safer means of studying wildlife in remote places compared to traditional surveys (Fretwell *et al.* 2014, LaRue *et al.* 2011). The cost of acquiring VHR satellite imagery has reduced in the past decade (Fretwell *et al.* 2014, LaRue *et al.* 2017), with discounts available for the nonprofit sector, particularly education (LaRue *et al.* 2017). The personnel and analysis time are roughly comparable between VHR satellite imagery and traditional surveys, although less personnel are usually required for satellite imagery analysis. However compared to the main cost of most traditional surveys (*i.e.*, fuel and charter of the survey platform), satellite imagery can be substantially cheaper, particularly for remote areas. A considerable advantage of using satellite imagery is that no time-consuming logistics and permitting are involved in this approach.

Conclusion

This survey is the first to address detection and species description (both visually and spectrally) of whales with WorldView-3 satellite imagery, suggesting that great whales can be detected on VHR satellite imagery. However, some species such as humpback whales and southern right whales were more difficult to detect on satellite images, although they are easily identifiable from boat or aerial surveys. This is due to either their body coloration being similar to their environment or to their behavior, which can make it difficult to discern body shape from above. The opposite is true for species with less acrobatic behavior at the surface, or lighter body coloration, such as fin and gray whales, which appear more easily discernible on satellite images in our study. VHR satellite technology could, therefore, be useful to monitor some whale species, especially over large areas of the ocean. Next steps in development of this approach will be (1) to automate or semiautomate

the detection of each species following methods by Fretwell *et al.* (2014), and using an object-based image analysis approach which is likely to be more appropriate based on this study findings; and (2) to compare sightings data from the VHR satellite imagery approach with data collected from traditional survey methods, to test the efficacy of high resolution satellite imagery for measuring population density. Downstream, this technique has the potential to be used to measure whale densities and assessment density changes through time, following a thorough review of how satellite imagery analysis compares with traditional surveys for making such measurements.

Acknowledgments

This research was possible thanks to the MAVA Foundation for their financial support of the project "Studying Whales from Space" (16035). We are also thankful to DigitalGlobe for providing us with satellite imagery. This study represents a contribution to the Ecosystems Component of the British Antarctic Survey Polar Science for Planet Earth Programme, funded by the Natural Environment Research Council (NERC). We are grateful for the thoughtful comments and reviews of the three anonymous referees, which greatly improved the manuscript.

Literature Cited

Abileah, R. 2002. Marine mammal census using space satellite imagery. U.S. Navy Journal of Underwater Acoustics 52:709–724.

Bailey, H., B. R. Mate, D. M. Palacios, L. Irvine, S. J. Bograd and D. P. Costa. 2009. Behavioural estimation of blue whale movements in the northeast Pacific from state-space model analysis of satellite tracks. Endangered Species Research 10:93–106.

Baird, R. W., Cholewiak, D., Webster, *et al.* 2015. Biologically Important Areas for cetaceans within U.S. waters – Hawai'i region. Pages 54–64 *in* S. M. Van Parijs, C. Curtice and M. C. Ferguson, eds. Biologically Important Areas for cetaceans within U.S. waters. Aquatic Mammals (Special Issue) 41(1).

Barlow, J. 2006. Cetacean abundance in Hawaiian waters estimated from a summer/fall survey in 2002. Marine Mammal Science 22:446–464.

Boisseau, O. 2014. Visual sightings from Song of the Whale 1993–2013. Data downloaded from OBIS-SEAMAP at http://seamap.env.duke.edu/dataset/1158.

Buckland, S. T., and B. J. Turnock. 1992. A robust line transect method. Biometrics 48:901–909.

Buckland, S. T., D. R. Anderson, K. P. Burnham, J. L. Laake, D. L. Borchers and L. Thomas. 2001. Introduction to distance sampling: Estimating abundance of biological populations. Oxford University Press, Oxford, U.K.

Calambokidis, J., and J. Barlow. 2004. Abundance of blue and humpback whales in the eastern North Pacific estimated by capture-recapture and line-transect methods. Marine Mammal Science 20:63–85.

Cerchio, S., B. Andrianantenaina, A. Lindsay, M. Rekdahl, N. Andrianarivelo and T. Rasoloarijao. 2015. Omura's whales (*Balaenoptera omurai*) off northwest Madagascar: Ecology, behaviour and conservation needs. Royal Society Open Science 2:150301.

Clapham, P. J., and C. S. Baker. 2002. Whaling, modern. Pages 1239–1243 *in* W. F. Perrin, B. Würsig and J. G. M. Thewissen, eds. Encyclopedia of marine mammals. Academic Press, New York, NY.

Clapham, P. J., and J. G. Mead. 1999. *Megaptera novaeangliae*. Mammalian Species 604:1–9.

Cooke, J., V. Rowntree and M. Sironi. 2015. Southwest Atlantic right whales: Interim updated population assessment from photo-id collected at Península Valdéz, Argentina. Paper SC/66a/BRG/23 presented to the IWC Scientific Committee (unpublished). 10 pp. Available at http://www.icb.org.ar/Publicaciones/10%20RS5602_SC_66a_BRG_23.pdf.

Crespo, E. A., S. N. Pedraza, S. L. Dans, M. A. Coscarella, G. M. Svendsen and M. Degrati. 2014. Number of southern right whales, *Eubalaena australis*, and population trend in the neighbourhood of Península Valdès during the period 1999–2013 by means of aerial and boat surveys. Paper SC/65-b/BRG07 presented to the IWC Scientific Committee (unpublished). 17 pp. Available at https://archive.iwc.int/pages/view.php?ref=5001&search=%21collection165&order_by=relevance&sort=DESC&offset=0&archive=0&k=&curpos=6&restypes=.

Dhermain, F., G. Astruc, C. Cesarini, *et al.* 2015. Recensement des échouages de cétacés sur les côtes françaises de Méditerranée, entre 2010 et 2012 [Survey of strandings of cetaceans on the French coasts of the Mediterranean, between 2010 and 2012]. Scientific Reports of Port-Cros National Park 29:103–126.

DigitalGlobe. 2017. WorldView-3. 2 pp. Available at dg-cms-uploads-production.s3.amazonaws.com/uploads/document/file/95/DG2017_WorldView-3_DS.pdf.

Donovan, G. P., and T. Gunnlaugsson. 1989. North Atlantic sightings survey 1987: Report of the aerial survey off Iceland. Report of the International Whaling Commission 39:437–441.

Forcada, J., G. Notarbartolo di Sciara and F. Fabbri. 1995. Abundance of fin whales and striped dolphins summering in the Corso-Ligurian Basin. Mammalia 59:127–140.

Frankel, A. S., C. W. Clark, L. M. Herman and C. M. Gabriele. 1995. Spatial distribution, habitat utilization, and social interactions of humpback whales, *Megaptera novaeangliae*, off Hawai'i, determined using acoustic and visual techniques. Canadian Journal of Zoology 73:1134–1146.

Frantzis, A., O. Nikolaou, J. Bompar and A. Cammedda. 2004. Humpback whale (*Megaptera novaeangliae*) occurrence in the Mediterranean Sea. Journal of Cetacean Research and Management 6:25–28.

Fretwell, P. T., I. J. Staniland and J. Forcada. 2014. Whales from space: Counting southern right whales by satellite. PLoS ONE 9(2):e88655.

Frey, S. 2015. OceanCare cetacean sightings 2001–2014. Data downloaded from OBIS-SEAMAP at http://seamap.env.duke.edu/dataset/662.

Groom, G., I. Krag Petersen, M. D. Anderson and A. D. Fox. 2011. Using object-based analysis of image data to count birds: Mapping of lesser flamingos at Kamfers Dam, Northern Cape, South Africa. International Journal of Remote Sensing 32:4611–4639.

Halpin, P., A. Read, E. Fujioka, *et al.* 2009. OBIS-SEAMAP: The world data center for marine mammal, sea bird, and sea turtle distributions. Oceanography 22:104–115.

Häussermann, V., C. S. Gutstein, M. Beddington, *et al.* 2017. Largest baleen whale mass mortality during strong El Niño event is likely related to harmful toxic algal bloom. PeerJ 5:e3123.

Helweg, D. A., and L. M. Herman. 1994. Diurnal patterns of behaviour and group membership of humpback whales (*Megaptera novaeangliae*) wintering in Hawaiian waters. Ethology 98:298–311.

Herman, L. M., A. A. Pack, K. Rose, A. Craig, E. Y. K. Herman, S. Hakala and A. Milette. 2011. Resightings of humpback whales in Hawaiian waters over spans of 10–32 years: Site fidelity, sex ratios, calving rates, female

demographics, and the dynamics of social and behavioral roles of individuals. Marine Mammal Science 27:736–768.

Hiby, A. R., and P. S. Hammond. 1989. Survey techniques for estimating abundance of cetaceans. Report of the International Whaling Commission (Special Issue 11):47–80.

Iñiguez, M. A. 2001. Seasonal distribution of killer whales (*Orcinus orca*) in northern Patagonia, Argentina. Aquatic Mammals 27:154–161.

IUCN (International Union for Conservation of Nature). 2017. The IUCN Red List of Threatened Species. Version 2017-1. IUCN, Gland, Switzerland.

IWC (International Whaling Commission). 2011. Report of the joint IWC-ACCOBAMS workshop on reducing risk of collisions between vessels and cetaceans. Report IWC/63/CC 8 presented to the IWC Conservation Committee (unpublished). 42 pp. Available at https://iwc.int/iwc63docs.

IWC (International Whaling Commission). 2013. Report of the IWC Workshop on the Assessment of Southern Right Whales. Journal of Cetacean Research and Management 14(Supplement):439–462.

IWC (International Whaling Commission). 2015. IWC/66/WK-WI-Rep01, report of the third workshop on large whale entanglement issues. Report SC/66-a/COMM/2 presented to the IWC Workshop on Large Whale Entanglement Issues (unpublished). 40 pp. Available at https://archive.iwc.int/pages/terms.php?k=&url=pages/collection_download.php?collection=220%26k=.

Jefferson, T. A., M. A. Webber, R. L. Pitman and U. Gorter. 2015. Marine mammals of the world: A comprehensive guide to their identification. Second edition. Academic Press, London, U.K.

Jones, M. L., and S. L. Swartz. 1984. Demography and phenology of gray whales and evaluation of whale-watching activities in Laguna San Ignacio, Baja California Sur, Mexico. Pages 309–374 *in* M. L. Jones, S. L. Swartz and S. Leatherwood, eds. The gray whale: *Eschrichtius robustus*. Academic Press, Orlando, FL.

Knowlton, A. R., P. K. Hamilton, M. K. Marx, H. M. Pettis and S. D. Kraus. 2012. Monitoring North Atlantic right whale *Eubalaena glacialis* entanglement rates: A 30 yr retrospective. Marine Ecology Progress Series 466:293–302.

Laist, D. W., A. R. Knowlton, J. G. Mead, A. S. Collet and M. Podestà. 2001. Collisions between ships and whales. Marine Mammal Science 17:35–75.

Lanfredi, C., and G. Notarbartolo di Sciara. 2011. Tethys Research Institute aerial survey cetacean sightings 2009-2011. Data downloaded from OBIS-SEAMAP at http://seamap.env.duke.edu/dataset/776.

Lanfredi, C., and G. Notarbartolo di Sciara. 2014. Tethys research institute shipboard survey cetacean sightings 1986–2012. Data downloaded from OBIS-SEAMAP at http://seamap.env.duke.edu/dataset/774.

LaRue, M. A., J. J. Rotella, R. A. Garrott, *et al*. 2011. Satellite imagery can be used to detect variation in abundance of Weddell seals (*Leptonychotes Weddellii*) in Erebus Bay, Antarctica. Polar Biology 34:1727–1737.

LaRue, M. A., S. Stapleton and M. Anderson. 2017. Feasibility of using high-resolution satellite imagery to assess vertebrate wildlife populations. Conservation Biology 31:213–220.

Learmonth, J. A., C. D. Macleod, M. B. Santos, G. J. Pierce, H. Q. P. Crick and R. A. Robinson. 2006. Potential effects of climate change on marine mammals. Oceanography and Marine Biology: An Annual Review 44:431–464.

Levy, R., D. Uminsky, A. Park and J. Calambokidis. 2011. A theory for the hydrodynamic origin of whale flukeprints. International Journal of Non-Linear Mechanics 46:616–626.

Maire, F., L. M. Alvarez and A. Hodgson. 2015. Automating marine mammal detection in aerial images captured during wildlife surveys: A deep learning approach. Pages 379-385 *in* B. Pfahringer and J. Renz, eds. AI 2015:

Advances in artificial intelligence. Lecture Notes in Computer Science, Volume 9457. Springer, Cham, Switzerland.

Marsh, H., and D. F. Sinclair. 1989. Correcting for visibility bias in strip transect aerial surveys of aquatic fauna. The Journal of Wildlife Management 53: 1017–1024.

Mate, B. R., and J. Urbán-Ramirez. 2003. A note on the route and speed of a gray whale on its northern migration from Mexico to central California, tracked by satellite-monitored radio tag. Journal of Cetacean Research and Management 5:155–157.

Mate, B., B. A. Lagerquist and J. Calambodikis. 1999. Movements of North Pacific blue whales during the feeding season off southern California and their southern fall migration. Marine Mammal Science 15:1246–1257.

McMahon, C. R., H. Howe, J. Van Den Hoff, R. Alderman, H. Brolsma and M. A. Hindell. 2014. Satellites, the all-seeing eyes in the sky: Counting elephant seals from space. PLoS ONE 9(3):e92613.

Mellinger, D. K., K. M. Stafford, S. E. Moore, R. P. Dziak and H. Matsumoto. 2007. An overview of fixed passive acoustic observation methods for cetaceans. Oceanography 20(4):36–45.

Mobley, J. R., S. S. Spitz, K. A. Forney, R. Grotefendt and P. H. Forestell. 2000. Distribution and abundances of odontocete species in Hawaiian waters: Preliminary results of 1993–98 aerial surveys. National Marine Fisheries Service Southwest Fisheries Science Center Administrative Report LJ-00-14C. 30 pp.

Mobley, J., S. Spitz and R. Grotefendt. 2001. Abundance of humpback whales in Hawaiian waters: Results of 1993–2000 aerial surveys. Report to the Hawaiian Islands Humpback Whale National Marine Sanctuary Office of National Marine Sanctuaries, NOAA, U.S. Department of Commerce, Department of Land and Natural Resources State of Hawaii. 17 pp.

Moulins, A., M. Rosso, M. Ballardini and M. Würtz. 2008. Partitioning of the Pelagos Sanctuary (north-western Mediterranean Sea) into hotspots and coldspots of cetacean distributions. Journal of the Marine Biological Association of the United Kingdom 88:1273–1281.

Nathans, J., D. Thomas and D. S. Hogness. 1986. Molecular genetics of human color vision: The genes encoding blue, green, and red pigments. Science 232:193–202.

Nieukirk, S. L., K. M. Stafford, D. K. Mellinger, R. P. Dziak and C. G. Fox. 2004. Low-frequency whale and seismic airgun sounds recorded in the Mid-Atlantic Ocean. Journal of the Acoustical Society of America 115: 1832–1843.

Notarbartolo di Sciara, G., M. Zanardelli, M. Jahoda, S. Panigada and S. Airoldi. 2003. The fin whale *Balaenoptera physalus* (L. 1758) in the Mediterranean Sea. Mammal Review 33:105–150.

Panigada, S., M. Zanardelli, M. MacKenzie, C. Donovan, F. Mélin and P. S. Hammond. 2008. Modelling habitat preferences for fin whales and striped dolphins in the Pelagos Sanctuary (western Mediterranean Sea) with physiographic and remote sensing variables. Remote Sensing of Environment 112:3400–3412.

Panigada, S., G. Lauriano, L. Burt, N. Pierantonio and G. Donovan. 2011. Monitoring winter and summer abundance of cetaceans in the Pelagos Sanctuary (northwestern Mediterranean Sea) through aerial surveys. PLoS ONE 6(7): e22878.

Payne, R. 1986. Long term behavioural studies of the southern right whale (*Eubalaena australis*). Report of the International Whaling Commission (Special Issue 10):161–167.

Perrin, W. F., B. G. Würsig and J. G. M. Thewissen. 2009. Encyclopedia of marine mammals. Second edition. Academic Press, London, U.K.

Pollock, K. H., H. D. Marsh, I. R. Lawler and M. W. Alldredge. 2006. Estimating animal abundance in heterogeneous environments: An application to aerial surveys for dugongs. Journal of Wildlife Management 70:255–262.

Ponce, D., A. M. Thode, M. Guerra, J. Urbán R and S. Swartz. 2012. Relationship between visual counts and call detection rates of gray whales (*Eschrichtius robustus*) in Laguna San Ignacio, Mexico. Journal of the Acoustical Society of America 131:2700–2713.

Ramp, C., J. Delarue, P. J. Palsbøll, R. Sears and P. S. Hammond. 2015. Adapting to a warmer ocean—seasonal shift of baleen whale movements over three decades. PLoS ONE 10(3):e0121374.

Rasmussen, K., D. M. Palacios, J. Calambokidis, *et al*. 2007. Southern hemisphere humpback whales wintering off Central America: Insights from water temperature into the longest mammalian migration. Biology Letters 3:302–305.

Rees, W. G. 2013. Physical principles of remote sensing. Third edition. Cambridge University Press, Cambridge, U.K.

Reeves, R. R., and T. D. Smith. 2003. A taxonomy of world whaling: Operations, eras, and data sources. Northeast Fisheries Science Centre Reference Document 03-12. 28 pp.

Reilly, S. B., J. L. Bannister, P. B. Best, *et al*. 2008. *Balaenoptera omurai*. The IUCN Red List of Threatened Species 2008:e.T136623A4319390.

Reilly, S. B., J. L. Bannister, P. B. Best, *et al*. 2013. *Balaenoptera physalus*. The IUCN Red List of Threatened Species 2013:e.T2478A44210520.

Rey, N., M. Volpi, S. Joost and D. Tuia. 2017. Detecting animals in African savanna with UAVs and the crowds. Remote Sensing of Environment 200: 341–351.

Robbins, W. D., V. M. Peddemors, S. J. Kennelly and M. C. Ives. 2014. Experimental evaluation of shark detection rates by aerial observers. PLoS ONE 9(2):e83456.

Rowntree, V. J., R. S. Payne and D. M. Schell. 2001. Changing patterns of habitat use by southern right whales (*Eubalaena australis*) on their nursery ground at Península Valdès, Argentina, and in their long-range movements. Journal of Cetacean Research and Management (Special Issue) 2:133–143.

Rugh, D. J., K. E. W. Shelden and A. Schulman-Janiger. 2001. Timing of the gray whale southbound migration (*Eschrichtius robustus*). Journal of Cetacean Research and Management 3:31–39.

Schumann, N., N. J. Gales, R. G. Harcourt and J. P. Y. Arnould. 2013. Impacts of climate change on Australian marine mammals. Australian Journal of Zoology 61:146–159.

Shirihai, H., and B. Jarrett. 2006. Whales, dolphins and seals: A field guide to the marine mammals of the world. A&C Black, London, U.K.

Silber, G. K., M. D. Lettrich, P. O. Thomas, *et al*. 2017. Projecting marine mammal distribution in a changing climate. Frontiers in Marine Science 4:1–14.

Smultea, M. A., T. A. Jefferson and A. M. Zoidis. 2010. Rare sightings of a Bryde's whale (*Balaenoptera edeni*) and sei whales (*B. borealis*) (Cetacea: Balaenopteridae) northeast of O'ahu, Hawai'i. Pacific Science 64:449–457.

Smultea, M., D. Fertl, C. Bacon, M. Moore, V. James and B. Wursig. 2017. Cetacean mother-calf behavior observed from a small aircraft off Southern California. Animal Behavior and Cognition 4:1–23.

Steiger, G. H., J. Calambokidis, R. Sears, K. C. Balcomb and J. C. Cubbage. 1991. Movement of humpback whales between California and Costa Rica. Marine Mammal Science 7:306–310.

Supriadi, I., and A. S. Prihatmanto. 2016. Design and implementation of Indonesia United portal using crowdsourcing approach for supporting conservation and monitoring of endangered species. Proceedings of the 2015 4th International Conference on Interactive Digital Media, ICIDM 2015.

Urbán, J., and A. Aguayo. 1987. Spatial and seasonal distribution of the humpback whale, *Megaptera novaeangliae*, in the Mexican Pacific. Marine Mammal Science 3:333–344.

Urbán, J., L. Rojas-Bracho, H. Pérez-Cortés, *et al.* 2003. A review of gray whales (*Eschrichtius robustus*) on their wintering grounds in Mexican waters. Journal of Cetacean Research and Management 5:281–295.

Vaes, T., and J-N. Druon. 2013. Mapping of potential risk of ship strike with fin whales in the western Mediterranean Sea: A scientific and technical review using the potential habitat of fin whales and the effective vessel density. Joint Research Centre of the European Commission Report EUR 25847EN. 28 pp. Available at https://europa.eu/.

Van Canneyt, O. 2016. Observatoire Pelagis aerial surveys 2002–2015. Data downloaded from OBIS-SEAMAP at http://seamap.env.duke.edu/dataset/1404.

Woodward, B. L., J. P. Winn and F. E. Fish. 2006. Morphological specializations of baleen whales associated with hydrodynamic performance and ecological niche. Journal of Morphology 267:1284–1294.

Yang, Z., T. Wang, A. K. Skidmore, J. De Leeuw, M. Y. Said and J. Freer. 2014. Spotting East African mammals in open savannah from space. PLoS ONE 9: e115989.

Received: 13 September 2017
Accepted: 8 July 2018

Supporting Information

The following supporting information is available for this article online at http://onlinelibrary.wiley.com/doi/10.1111/mms.12544/suppinfo.

Appendix S1. Classification method and validation.

Table S1. List of parameters to identify whale-like objects on satellite images based on Jefferson *et al.* (2015) and Woodward *et al.* (2006). The minimum values for "body length range" corresponds to size of calves. The maximum values for "body length range" corresponds to the maximum length of an adult.

Table S2. Classification score equation and categorization for the studied species: gray whale, southern right whale, humpback whale and fin whale. Some classification parameters (Table S1) were down-weighted, if there was less than 75% consensus. Other parameters, characteristic of whales (*i.e.*, flukeprint, fluke and flipper), where up-weighted only if more than 75% consensus was reached. For fin whales, the flukeprint parameter had to be down-weighted, as it reached less than 75% consensus (Table S3).

Table S3. Percentage of consensus reached for each parameter listed in Table S1 per species.

Table S4. Results of the classification score and categorization comparison between the three observers, including the consensus for the categorization.

Appendix S2. List of pixel descriptions for whales.

Appendix S3. Recommendation matrix concerning which large whale species might be ideal candidates for VHR satellite surveys based on species information from Shirihai and Jarrett (2006), and Jefferson *et al.* (2015). Note that this matrix does not consider the possibility of cooccurrence with similar species, as this aspect varies between localities for each species.